Gains For RF Tags Using Multiple Antennas

Joshua D. Griffin, *Student Member, IEEE*, and Gregory D. Durgin, *Senior Member, IEEE*

Abstract—Backscatter radio systems, including high frequency radio frequency identification (RFID), operate in the *dyadic backscatter channel*—a two-way pinhole channel that has deeper small-scale fades than that of a conventional one-way channel. This paper shows that *pinhole diversity* is available in a rich scattering environment caused by modulating backscatter with multiple RF tag antennas—no diversity combining at the reader, channel knowledge, or signaling scheme change is required. Pinhole diversity, along with increased RF tag scattering aperture, can cause up to a 10 dB reduction in the power required to maintain a constant bit-error-rate for an RF tag with two antennas. Through examples, it is shown that this gain results in increased backscatter radio system communication reliability and up to a 78% increase in RF tag operating range.

Index Terms—Dyadic backscatter channel, modulated backscatter, pinhole channel, pinhole diversity, probability, radio frequency identification (RFID), RF tag, radio link budget.

I. INTRODUCTION

THE use of modulated backscatter as a means of communication was originally proposed by Stockman in 1948 [1]. Since then, many compelling applications of modulated backscatter transponders, or RF tags, have emerged including radio frequency identification (RFID), passive sensors, and passive data transmission devices. RF tags consume little-to-no power from the incident signal and can be made extraordinarily small and inexpensive because backscatter modulation does not require the modulated signal to be amplified and retransmitted. Instead, as shown in Fig. 1, the RF tag simply scatters a portion of the incident continuous wave signal from the reader transmitter back to the reader receiver using load modulation—i.e., varying the complex antenna load reflection coefficient, $\tilde{\Gamma}(t)$, by switching the RF tag antenna load between two or more states [2].

RF tags pose numerous design challenges; of which, the need for increased operating range and reliability with minimum cost and complexity is foremost. Therefore, researchers have been forced to reconsider basic propagation assumptions in backscatter channels. In particular, small-scale fading in these channels can have *radically* different statistical properties than those in a conventional one-way wireless channel, resulting in deeper fades [3]. Even though backscatter channels often exhibit line-of-site (LOS) propagation, heavy small-scale fading will still be present due to indoor operation, a cluttered reader
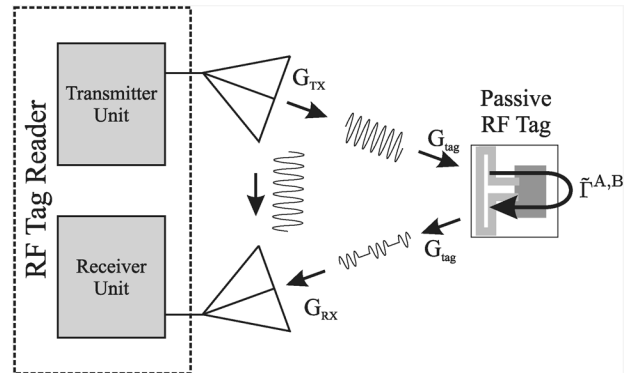

Fig. 1. In a far-field backscatter radio system, the reader transmits a continuous wave signal to the RF tag, which is typically modulated using load modulation, and scattered back to the receiver of the reader.

environment, and the inhomogeneous nature of the tagged objects. Such fading conditions, which severely limit RF tag range and reliability, can be overcome with diversity or coding techniques, but at the expense of increased complexity due to diversity combining and channel estimation. However, *pinhole diversity* gains are available to RF tags with more than one antenna that do not require this added complexity. Pinhole diversity gains only require multiple RF tag antennas and result in an improved channel envelope probability density function (PDF) which contributes to improved backscatter radio communication.

After outlining the mathematical model and PDF of the dyadic backscatter channel in Sections II and III, respectively, this paper demonstrates pinhole diversity gains using analytic envelope PDF expressions and bit-error-rate (BER) simulations in Section IV. In Section V, it is shown that pinhole diversity gains contribute up to a 10 dB BER gain (for a BER of 10^{-4}) resulting in up to a 78% increase in RF tag range in a free space environment. Pinhole diversity gains can be exploited in real backscatter radio systems using the design guidelines presented in Section V.

II. $M \times L \times N$ DYADIC BACKSCATTER CHANNEL

The most general backscatter channel is the $M \times L \times N$ dyadic[1] *backscatter channel*—a pinhole channel [4] that describes the propagation of signals in a backscatter radio system consisting of M transmitter, L RF tag, and N receiver antennas. In a pinhole channel, propagation paths are forced to converge at a point reducing the rank of the channel matrix which has been shown to decrease the capacity available in the channel [4]. In RF channels, the point of convergence may be a diffracting

The authors are with the School of Electrical and Computer Engineering, Georgia Institute of Technology (Georgia Tech), Atlanta, GA 30332 USA (e-mail: jdgriffin@ieee.org).

[1]The term "dyadic" has a double meaning. It reflects both the two-fold nature of the channel created by the forward and backscatter links and the fact that the modulated signals are represented in matrix form.
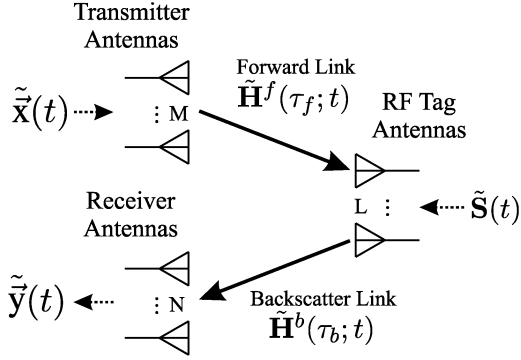
Fig. 2. The general $M \times L \times N$ dyadic backscatter channel with M transmitter antennas, L RF tag antennas, and N receiver antennas described mathematically by (1).

edge [5], [6], a hallway or tunnel [5], a metal screen [4], rings of scatterers separated by a long distance [7], or the antenna(s) of a mobile station that is (are) found in amplify-and-forward channels [8]. In the dyadic backscatter channel, the point of convergence is the RF tag antenna(s). All of these pinhole channels, except the amplify-and-forward and dyadic backscatter channels, cease their pinhole behavior under line-of-sight (LOS) conditions. The dyadic backscatter and amplify-and-forward channels remain pinholes in both LOS and non-line-of-site (NLOS) conditions making them some of the only true pinhole channels.

The hallmark of any pinhole channel is that it can be modeled as the cascade of two channels. In the $M \times L \times N$ dyadic backscatter channel, shown in Fig. 2, these channels are called the forward and backscatter links. The forward link, $\tilde{\mathbf{H}}^f$, describes signal propagation from M transmitter antennas to L RF tag antennas and the backscatter link, $\tilde{\mathbf{H}}^b$, describes the propagation of signals scattered from L RF tag antennas to N receiver antennas.

In mathematical terms, the received, baseband signal from the $M \times L \times N$ dyadic backscatter channel is

$$\tilde{\mathbf{y}}(t) = \frac{1}{2} \int_{-\infty}^{+\infty} \int_{-\infty}^{+\infty} \tilde{\mathbf{H}}^b(\tau_b;t)\tilde{\mathbf{S}}(t)\tilde{\mathbf{H}}^f(\tau_f;t)$$
$$\times \tilde{\mathbf{x}}(t - \tau_b - \tau_f)d\tau_b d\tau_f + \tilde{\mathbf{n}}(t). \quad (1)$$

In (1), $\tilde{\mathbf{y}}(t)$ is an $N \times 1$ vector of received, baseband signals; $\tilde{\mathbf{H}}^b(\tau_b;t)$ is the $N \times L$, complex, baseband channel impulse response matrix of the backscatter link; and $\tilde{\mathbf{H}}^f(\tau_f;t)$ is the $L \times M$, complex, baseband channel impulse response matrix of the forward link [9]. $\tilde{\mathbf{S}}(t)$ is the tag's narrowband $L \times L$ signaling matrix, $\tilde{\mathbf{x}}(t)$ is an $M \times 1$ vector of signals transmitted from the transmitter antennas, and $\tilde{\mathbf{n}}(t)$ is an $N \times 1$ vector of noise components. This channel has been investigated by Ingram *et al.* [10] in the context of RFID systems using active[2] RF tags. Ingram *et al.* was the first to propose the use of multiple antennas at both the reader and RF tag for transmit diversity and spatial multiplexing to increase the range and communication capacity, respectively. Mi *et al.* also advocates the use of multiple RF

tag antennas for the purpose of increasing the power available to the RF tag integrated circuit (IC) [11]. Kim *et al.* [3] has conducted narrowband channel measurements at 2.4 GHz of a $1 \times 1 \times 1$ dyadic backscatter channel calculating the cumulative density function (CDF) and path loss exponent of the channel in an indoor office environment.

A. The Signaling Matrix

The signaling matrix, $\tilde{\mathbf{S}}(t)$, is an $L \times L$ matrix that describes the time-varying modulation that an RF tag places on radio signals absorbed and scattered by the L tag antennas. Therefore, it is natural to define the signaling matrix as the L port scattering matrix commonly used in RF hardware design. A comprehensive discussion of the general L port scattering matrix is given by Pozar [12]. However, two notes are worth mentioning. First, the signaling matrix of a passive or active RF tag has elements $\tilde{\mathbf{s}}_{ij}(t)$ with magnitude less than unity, $|\tilde{\mathbf{s}}_{ij}(t)| \leq 1$, since there is no amplification of the backscattered signal. Second, though it is not required that the signaling matrix be symmetric, most RF tags will satisfy this property.

The signaling matrix may take several different forms depending upon the physical implementation of the modulation circuitry and RF tag antennas.

1) Identity Signaling Matrix: If each RF tag antenna is used to modulate backscatter with the same signal and no signals are transferred between the antennas, the signaling matrix is the normalized identity matrix

$$\tilde{\mathbf{S}}(t) = \tilde{\mathbf{s}}(t)\mathbf{I}_{\mathrm{L}} = \tilde{\Gamma}(t)\mathbf{I}_{\mathrm{L}} \quad (2)$$

where $\mathbf{I}_{\mathrm{L}}$ is the $L \times L$ identity matrix and $\tilde{\Gamma}(t)$ is the complex, RF tag antenna load reflection coefficient.

2) Diagonal Signaling Matrix: If the RF tag antennas modulate backscatter with different signals and no signals are transferred between the antennas, the signaling matrix is a diagonal matrix

$$\tilde{\mathbf{S}}(t) = \mathrm{diag}\left[\tilde{\mathbf{s}}_{11}(t) \ldots \tilde{\mathbf{s}}_{LL}(t)\right]$$
$$= \mathrm{diag}\left[\tilde{\Gamma}_1(t) \ldots \tilde{\Gamma}_{\mathrm{L}}(t)\right]. \quad (3)$$

3) Full Signaling Matrix: If the RF tag antennas modulate backscatter independently and signals are transferred between the antennas, the full signaling matrix

$$\tilde{\mathbf{S}}(t) = \begin{bmatrix} \tilde{\mathbf{s}}_{11}(t) & \ldots & \tilde{\mathbf{s}}_{1L}(t) \\ \vdots & \ddots & \vdots \\ \tilde{\mathbf{s}}_{L1}(t) & \ldots & \tilde{\mathbf{s}}_{LL}(t) \end{bmatrix} \quad (4)$$

is used. Signal transfer between antennas is represented by the off diagonal elements (i.e., $\tilde{\mathbf{s}}_{ij}$ where $i \neq j$). The fact that power can be transferred between the RF tag antennas gives the designer a potential additional degree of freedom in signal scheme design; however, at this point, no application of the full signaling matrix has been identified.

For the remainder of this paper, it is assumed that the signaling matrix has the form of (2), the identity signaling matrix,
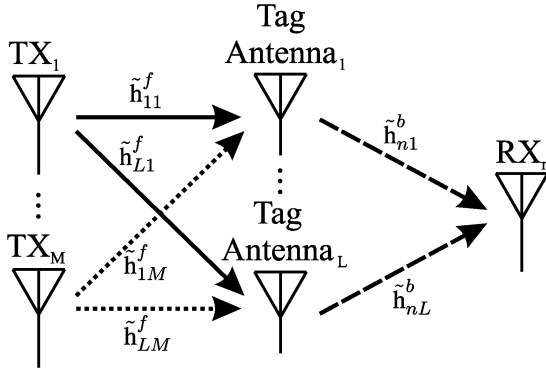
---

[2]A passive RF tag operates its circuitry using power rectified from the incident wave transmitted by the reader while an active tag uses a small battery or other onboard power source.

Fig. 3. In a backscatter radio system, the signal received at the nth receiving antenna is the sum of ML Gaussian products. However, only L of these products are statistically independent.

with binary reflection of signals, $\tilde{\Gamma} = \pm 1$, to provide maximum signal power.

III. $M \times L \times N$ Dyadic Backscatter Channel Envelope PDF

In a typical $M \times L \times N$ dyadic backscatter channel, LOS propagation dominates and the elements of the forward and backscatter matrices follow a Rician distribution. To investigate the lower bound of this case, NLOS propagation is assumed so that the elements of each link matrix are Rayleigh distributed. Consequently, each element of $\tilde{\mathbf{H}}^f$ and $\tilde{\mathbf{H}}^b$ is an independent, identically distributed (i.i.d.), zero-mean, complex Gaussian random variable. The elements of the backscatter and forward links can be written, respectively, as $\tilde{\mathbf{h}}^b = (w_b + jv_b)$ and $\tilde{\mathbf{h}}^f = (w_f + jv_f)$ where $w_{f,b}$ and $v_{f,b}$ are $\sim \mathcal{N}(0, \sigma_{f,b}^2/2)$. In this channel model, propagation paths that originate or terminate on a common RF tag antenna can have link correlation, ρ [13]. Mathematically, this means that $2\mathrm{Cov}(w_f, w_b)/\sigma_b\sigma_f = 2\mathrm{Cov}(v_f, v_b)/\sigma_b\sigma_f = \rho$ where $\mathrm{Cov}(\cdot, \cdot)$ is the covariance operator. The signal received at the nth receiver antenna is proportional to the sum of ML complex Gaussian products, described by (5) and Fig. 3

$$\tilde{y}_n(t) \propto \sum_{j=1}^{L} \underbrace{\left(\tilde{\mathbf{h}}_{j1}^f + \ldots + \tilde{\mathbf{h}}_{jM}^f \right)}_{\tilde{g}_j^f} \tilde{\mathbf{h}}_{nj}^b. \tag{5}$$

In (5), each element of the backscatter link matrix, $\tilde{\mathbf{h}}_{nj}^b$, is multiplied by M independent, identically distributed (i.i.d.) forward link elements, $(\tilde{\mathbf{h}}_{j1}^f + \ldots + \tilde{\mathbf{h}}_{jM}^f)$, which can be expressed as a single complex Gaussian random variable, $\tilde{g}_j^f$, with zero mean and variance $M\sigma_f^2$. Therefore, the signal received at the nth receiver antenna is proportional to the sum of L i.i.d. complex Gaussian products. With this understanding, the envelope PDF of the $M \times L \times N$ dyadic backscatter channel, $f_\alpha(\alpha, \rho)$, can be derived from that of the product of two Rayleigh random variables as shown in the Appendix. Two special cases of $f_\alpha(\alpha, \rho)$ are of interest: that with independent forward and backscatter links ($\rho = 0$) and that with fully

correlated forward and backscatter links ($\rho = 1$). The envelope PDF for the case of $\rho = 0$ is

$$f_\alpha(\alpha, 0) = \alpha^L \left(\frac{2}{\sqrt{M}\sigma_b\sigma_f} \right)^{1+L} \frac{2^{1-L}}{\Gamma(L)} K_\nu \left(\frac{2\alpha}{\sqrt{M}\sigma_b\sigma_f} \right) \tag{6a}$$

where α is the channel envelope, $\Gamma(\cdot)$ is the gamma function, and $K_\nu(\cdot)$ is a modified bessel function of the second kind with order $\nu = 1 - L$. The mean and variance of (6a), respectively, are

$$\mu_\alpha = \frac{\sqrt{M}\sigma_b\sigma_f}{2} \frac{\pi(2L)!}{4^L L!(L-1)!} \tag{6b}$$

and

$$\sigma_\alpha^2 = ML\sigma_b^2\sigma_f^2 \left(1 - \frac{L}{4} \left[\frac{\pi(2L)!}{4^L(L!)^2} \right]^2 \right). \tag{6c}$$

The envelope PDF for the case of $\rho = 1$, which may occur only in a $1 \times L \times 1$ dyadic backscatter channel in which a single reader antenna is used to transmit and receive, is

$$f_\alpha(\alpha, 1) = \alpha^{L/2} \left(\frac{1}{\sigma_b\sigma_f} \right)^{1+L/2} \frac{2^{1-L/2}}{\Gamma(L/2)} K_\nu \left(\frac{\alpha}{\sigma_b\sigma_f} \right) \tag{7a}$$

where $K_\nu(\cdot)$ is a modified bessel function of the second kind with order $\nu = 1 - L/2$ and all other terms are as defined for (6a). The mean and variance of (7a), respectively, are

$$\mu_\alpha = \sigma_b\sigma_f \Psi \tag{7b}$$

where

$$\Psi = \begin{cases} \frac{\pi L!}{2^L (L/2-1)!(L/2)!} & \text{for even } L \\ \frac{2^L [(L/2-1/2)!]^2}{2(L-1)!} & \text{for odd } L \end{cases}$$

and

$$\sigma_\alpha^2 = 2L\sigma_b^2\sigma_f^2 \left(1 - \frac{\Lambda}{2L} \right) \tag{7c}$$

where

$$\Lambda = \begin{cases} \left[\frac{\pi L!}{2^L (L/2)!(L/2-1)!} \right]^2 & \text{for even } L \\ \left[\frac{2^{L-1}[(L/2-1/2)!]^2}{(L-1)!} \right]^2 & \text{for odd } L. \end{cases}$$

Table I and Table II give simplified forms of (6a)–(6c) and (7a)–(7c), respectively, for common values of L.

IV. Diversity Gains in the Dyadic Backscatter Channel

A. The Benefits of Multiple RF Tag Antennas

Fig. 4 shows plots of (6a) and (7a) along with the PDF of a conventional one-way Rayleigh fading channel. Each PDF has been normalized to unit power, that is, $\mathcal{E}\{\alpha^2\} = 1$ where $\mathcal{E}\{\cdot\}$ denotes the ensemble average. In Fig. 4, it can be seen that the

TABLE I
SIMPLIFIED ENVELOPE STATISTICS FOR THE $M \times L \times N$ DYADIC BACKSCATTER CHANNELS WITH INDEPENDENT ($\rho = 0$), RAYLEIGH FADING LINKS

	$f_\alpha(\alpha, 0)$	μ_α	σ_α^2
$L = 1$	$\dfrac{4\alpha}{\zeta^2} \mathrm{K}_0\left(\dfrac{2\alpha}{\zeta}\right)$	$\dfrac{\pi}{4}\zeta$	$\left(1 - \dfrac{\pi^2}{16}\right)\zeta^2$
$L = 2$	$\dfrac{4\alpha^2}{\zeta^3} \mathrm{K}_{-1}\left(\dfrac{2\alpha}{\zeta}\right)$	$\dfrac{3\pi}{8}\zeta$	$\left(2 - \dfrac{9\pi^2}{64}\right)\zeta^2$
$L = 3$	$\dfrac{2\alpha^3}{\zeta^4} \mathrm{K}_{-2}\left(\dfrac{2\alpha}{\zeta}\right)$	$\dfrac{15\pi}{32}\zeta$	$\left(3 - \dfrac{225\pi^2}{1024}\right)\zeta^2$
$L = 4$	$\dfrac{2\alpha^4}{3\zeta^5} \mathrm{K}_{-3}\left(\dfrac{2\alpha}{\zeta}\right)$	$\dfrac{35\pi}{64}\zeta$	$\left(4 - \dfrac{1225\pi^2}{4096}\right)\zeta^2$

where $\quad \zeta = \sqrt{M}\sigma_b\sigma_f$

TABLE II
SIMPLIFIED ENVELOPE STATISTICS FOR THE $1 \times L \times 1$ DYADIC BACKSCATTER CHANNELS WITH FULLY CORRELATED ($\rho = 1$), RAYLEIGH FADING LINKS

	$f_\alpha(\alpha, 1)$	μ_α	σ_α^2
$L = 1$	$\dfrac{1}{\delta}\exp\left(\dfrac{-\alpha}{\delta}\right)$	δ	δ^2
$L = 2$	$\dfrac{\alpha}{\delta^2}\mathrm{K}_0\left(\dfrac{\alpha}{\delta}\right)$	$\dfrac{\pi}{2}\delta$	$4\delta^2\left(1 - \dfrac{\pi^2}{16}\right)$
$L = 3$	$\sqrt{\dfrac{2\alpha^3}{\pi\delta^5}}\mathrm{K}_{-1/2}\left(\dfrac{\alpha}{\delta}\right)$	2δ	$2\delta^2$
$L = 4$	$\dfrac{\alpha^2}{2\delta^3}\mathrm{K}_{-1}\left(\dfrac{\alpha}{\delta}\right)$	$\dfrac{3\pi}{4}\delta$	$8\delta^2\left(1 - \dfrac{18\pi^2}{256}\right)$

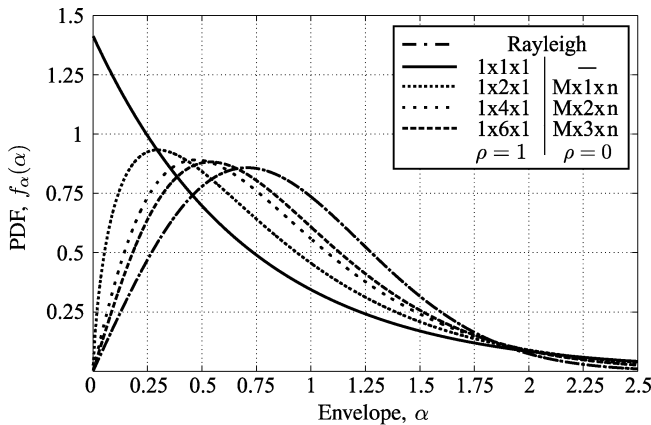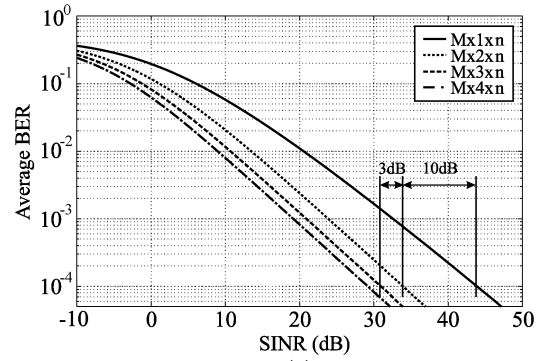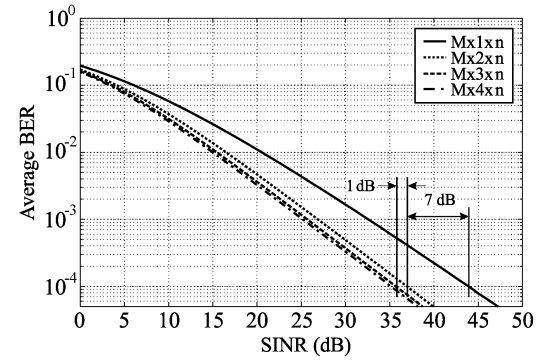where $\quad \delta = \sigma_b\sigma_f$

Fig. 4. Plots of the envelope PDF at the nth receiver antenna, with $\rho = 0$ and $\rho = 1$, for several dyadic backscatter channels along with the PDF of a conventional one-way Rayleigh fading channel. Each PDF has been normalized to unit power, that is, $\mathcal{E}\{\alpha^2\} = 1$ where $\mathcal{E}\{\cdot\}$ denotes the ensemble average.

Fig. 5. Average BER plots for backscatter radio systems operating in various dyadic backscatter channels with independent, Rayleigh fading forward and backscatter links, uncoded BPSK modulation, and noise and interference that is additive, white, and Gaussian. Each curve represents the average BER of the signal received at the nth reader receiver antenna with no diversity combining. Each BER curve is plotted against the SINR at the nth reader receiver antenna in the $1 \times 1 \times 1$ channel. In (a), the simulated random channel matrix is normalized by M for constant transmit power and the evident BER improvements are caused by both pinhole diversity gains and increased tag scattering aperture as RF tag antennas are added. In (b), the simulated random channel matrix is normalized by ML to show the BER improvements caused solely by pinhole diversity gains.

PDF of the dyadic backscatter channel has deeper fades than that of the one-way Rayleigh channel, but improves as RF tag antennas are added. The most significant change is seen for the fully correlated channel, $\rho = 1$, where the PDF changes from an exponential distribution for the $1 \times 1 \times 1$ channel to a product Rayleigh distribution for the $1 \times L \times 1$ channel ($L > 1$).

Improvements as RF tag antennas are added can also be seen in Fig. 5(a) which plots simulated average BER curves for various dyadic backscatter channels with independent, Rayleigh fading forward and backscatter links. The simulations use un-coded, coherent, binary phase shift keying (BPSK) modulation with noise and interference that is additive, white, and Gaussian. In these Monte Carlo simulations, 69×10^6 channel realizations were used to approximate the ensemble average of the BER and the simulated random channel matrix was normalized by the number transmit antennas, M, for constant transmit power. As RF tag antennas are added, the slopes of the BER curves increase and the curves are shifted in a manner similar to that caused by conventional diversity and coding techniques. For a BER of 10^{-4}, there is a 10 dB gain from the $1 \times 1 \times 1$ channel to the $1 \times 2 \times 1$ channel, with slightly larger gains for the $L = 3$ and $L = 4$ cases.

B. Pinhole Diversity Gains

The underlying physical process that yields the PDF improvements in Fig. 4 and contributes to the communication gains in Fig. 5(a) is a pinhole diversity gain caused by the use of multiple RF tag antennas. The term *pinhole diversity* is derived from the fact that each RF tag antenna corresponds to a pinhole in the channel that provides a set of spatially separated propagation paths, or pinhole diversity branches. Equation (5) shows

that, for the RF tag with L antennas, L diversity branches are formed by independent Gaussian product terms of the pinhole dyadic backscatter channel. As L increases, the probability that the envelope will fade is reduced and, as L becomes very large, it can be shown that the derived channel distributions become Gaussian with a Rayleigh distributed envelope.

Since pinhole diversity does not require diversity branch combining at the reader, it is often assumed that it is equivalent to diversity combining without channel knowledge in a one-way channel—i.e., the non-coherent addition of diversity branches received through a one-way channel at the receiver. However, pinhole diversity differs from both non-coherent diversity combining and conventional coherent diversity combining in two important aspects.

1) PDF Shape Change: Noncoherent diversity branch combining in a one-way Rayleigh fading channel only increases the power (or variance) of the received signal. Pinhole diversity gains, on the other hand, are caused by the summation of terms that have a product Rayleigh distribution resulting in a favorable change in the shape of the channel distribution. This can be seen in Fig. 4 where each PDF has been normalized to unit power.[3]

2) Reader Design Simplification: In a one-way channel, gain combining, switch combining, or gain combining in conjunction with space-time block codes must be used to affect a favorable change in the PDF shape. Pinhole diversity gains, on the other hand, can be realized in the dyadic backscatter channel using *only* multiple RF tag antennas to modulate backscatter—no change in the reader receiver hardware, reader transmitter hardware, or signaling scheme is required.

It should be noted that as Rayleigh products are summed, the power of the channel distribution does increase and can be attributed to an increase in the RF tag effective scattering aperture as antennas are added. This increase in scattered power can itself result in improved BER performance [10]. The BER plot shown in Fig. 5(a) reflects both this increase in effective scattering aperture and improved PDF shape caused by pinhole diversity. To see the BER improvement caused solely by pinhole diversity, the simulated random channel matrix has been normalized by ML, in Fig. 5(b), so that the channel power is held constant with respect to both M and L. Fig. 5(b) shows that pinhole diversity alone causes a 7 dB and 8 dB gain for the $1 \times 2 \times 1$ and $1 \times 3 \times 1$ channels, respectively, compared to the $1 \times 1 \times 1$ channel. Actual communication gains in a backscatter radio system are due to both pinhole diversity gains and increased effective scattering aperture; therefore, all performance comparisons should be based on Fig. 5(a).

C. Conventional Diversity Gains

As discussed previously, pinhole diversity causes the shape of the channel envelope PDF to change favorably and contributes to BER improvements; however, if conventional diversity combining techniques are used at the reader, even greater gains are available. Fig. 6 shows average BER curves for backscatter radio systems using maximal ratio combining (MRC), the optimum diversity combining technique for a fading channel,

[3]To judge whether or not the shape of the PDF has changed, comparisons must be made between distributions with equal channel power.
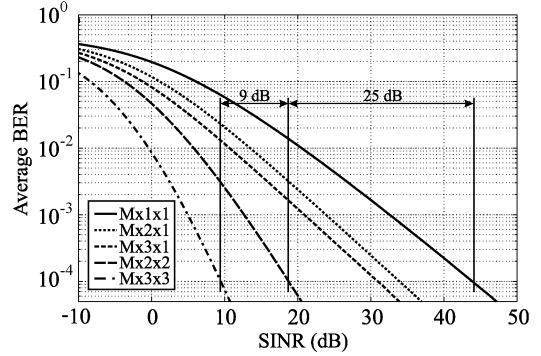

Fig. 6. Average BER plots for backscatter radio systems operating in various dyadic backscatter channels with independent Rayleigh fading forward and backscatter links, uncoded BPSK modulation, and noise and interference that is additive, white, and Gaussian. Each curve represents the average BER of the received signal using MRC with perfect channel knowledge at the reader receiver. The random channel matrix used in this simulation has been normalized by M for constant total transmit power. Each BER curve is plotted against the SINR at the nth reader receiver antenna in the $1 \times 1 \times 1$ channel.

at the reader receiver. No diversity combining is performed at the RF tag. In these Monte Carlo simulations, 69×10^6 channel realizations were used to approximate the ensemble average of the BER and the receiver had perfect knowledge of the independent, Rayleigh fading forward and backscatter links. Comparison of the BER plots for the $M \times L \times 1$ channel in Fig. 5(a) and Fig. 6 shows that MRC offers no further improvement over that caused by pinhole diversity gains (and increased scattering aperture), since the $M \times L \times 1$ channel offers only a single diversity branch to the MRC combiner at the reader receiver. However when $N > 1$, MRC gains and pinhole diversity gains combine for a significant communication performance improvement. At a BER of 10^{-4}, the $M \times 2 \times 2$ and $M \times 3 \times 3$ channels show up to a 25 dB and 34 dB gain with respect to the $1 \times 1 \times 1$ channel, respectively. These gains are caused by a power gain due to the increased RF tag scattering aperture, an improved PDF due to pinhole diversity, and maximal ratio combining.

D. Discussion

The analysis of this section has assumed that the envelope of the received signal at each antenna is uncorrelated. However, in any real antenna array, envelope correlation will exist as a function of the element spacing, electromagnetic coupling between array elements, and the angle spectrum of the multipath waves [9]. In a rich scattering environment, such correlation can be reduced at the reader by separating array elements by at least $\lambda/2$ [14]; however, footprint constraints may require smaller spacing of RF tag antennas resulting in higher envelope correlation and reduced pinhole diversity gain. At very worse, RF tag antenna envelope correlation will reduce the $M \times L \times N$ dyadic backscatter channel to an effective $M \times 1 \times N$ channel with added power due to the increased RF tag scattering aperture. Fortunately, research shows that diversity antennas with less than $\lambda/2$ spacing can also have low envelope correlation [15], [16]. Even in the case where pinhole diversity fails, MRC combining at the reader can be used to increase the RF tag range and reliability.

V. PRACTICAL BENEFITS AND DESIGN GUIDELINES

A. Backscatter Communication Radio Link Budget

In a backscatter radio system, the received signal is the sum of the desired modulated backscatter signal and a noise term that represents both noise and interfering signals. The ratio of their powers, the signal-to-interference-plus-noise ratio (SINR), determines the performance of the system. The power of the modulated backscatter signal can be calculated from the following backscatter communication radio link budget, modified from that given by Griffin *et al.* [17]

$$P_{\mathrm{rx}} = P_{\mathrm{tx}} - L_{\mathrm{sys}} + G_{\mathrm{tx}} + G_{\mathrm{rx}} + 20 \log_{10} \left(\left| [\tilde{\Gamma}^{\mathrm{A}} - \tilde{\Gamma}^{\mathrm{B}}]/2 \right| \right)$$
$$+ 2G_{\mathrm{tag}} - 2GP - 40 \log_{10} \left(\frac{4\pi}{\lambda} \right) - 40 \log_{10}(d) \quad (8)$$

where P_{tx} (dBm) is the power transmitted from the reader transmitter antennas, and G_{tx} (dBi) and G_{rx} (dBi) are the gains of the reader transmitter and receiver antennas, respectively. G_{tag} (dBi) is the RF tag antenna gain in free space; GP (dB) is a gain penalty due to material attachment; L_{sys} represents system losses in both the reader and RF tag; $40 \log_{10}(4\pi/\lambda)$ is a loss dependent upon the free space wavelength, λ; and $40 \log_{10}(d)$ is the free space path loss referenced to 1 m. In this case, d (m) is the total distance from the reader transmitter to the RF tag and back to the reader receiver. The power received at the reader, P_{rx} (dBm), with the DC component removed, is dependent upon the difference between two modulation states, $\tilde{\Gamma}^{\mathrm{A}}$ and $\tilde{\Gamma}^{\mathrm{B}}$, where

$$\tilde{\Gamma}^{\mathrm{A,B}} = \left(\tilde{Z}_{\mathrm{load}}^{\mathrm{A,B}} - \tilde{Z}_{\mathrm{antenna}}^* \right) / \left(\tilde{Z}_{\mathrm{load}}^{\mathrm{A,B}} + \tilde{Z}_{\mathrm{antenna}} \right) \quad (9)$$

and $(\cdot)^*$ is the complex conjugate. The practical benefit of using multiple RF tag antennas is the increased reliability and range of the backscatter radio system, demonstrated by the following two examples.

1) Reliability: Suppose that the RF tag is at a fixed distance from the reader such that there is adequate power to operate a passive RF tag (no such limitation is required for an active tag). If the channel worsens, by the introduction of interfering signals or increased fading from additional scatterers, the SINR at the reader may drop below the threshold required for successful detection of the signal. This may happen even though the passive RF tag is still powered. As Fig. 5(a) shows, an RF tag using multiple antennas will have a lower SINR threshold for a given BER. For a BER of 10^{-4}, the threshold is 10 dB lower for an RF tag using two antennas to modulate backscatter than for an RF tag using one antenna—a significant reliability increase.

2) Range: Suppose that all parameters of the channel are held constant and the distance of the RF tag from the reader is allowed to vary. As d increases, (8) dictates that the SINR will decrease and, at some distance, will fall below the threshold required to maintain a target BER. Using multiple RF tag antennas lowers this threshold allowing d to increase further without exceeding the desired BER. For a backscatter radio system using 2 RF tag antennas and a BER of 10^{-4}, a 10 dB gain is available resulting in up to a 78% increase in the range of the RF tag. This result was calculated using (8).

The 10 dB gain used the previous examples may be reduced in an actual $1 \times 2 \times 1$ channel since the target BER may be greater than 10^{-4}, indoor path loss may be larger or smaller than free space path loss [assumed in (8)], and the statistics of interfering signals may not be white and Gaussian [assumed in Fig. 5(a)]. Even so, since the source of this gain (i.e., the pinhole diversity gain coupled with an increased RF tag scattering aperture) only requires uncorrelated signal envelopes at the backscatter radio system antennas, multiple RF tag antennas will provide gains regardless of assumptions about path loss and interference-plus-noise statistics.

For passive RF tags, the range increase caused by multiple RF tag antennas will be limited by the RF tag chip sensitivity, i.e., the amount of power required to operate the tag circuitry [18]. Such a limit does not apply to active tags, since the power to operate the tag circuitry is drawn from an onboard power source. As RF tag power efficiency, which is strongly dependent upon the design of the tag's RF circuitry [19], improves, the limitation posed by chip sensitivity will decrease.

B. Backscatter Radio System Design Guidelines

Based on this analysis, the RF tag designer can exploit both pinhole diversity gains and conventional diversity gains at the reader by applying the following design guidelines.

1) Multiple RF Tag Antennas: The gains discussed in this paper are only available to RF tags with more than one antenna. Fig. 4 and Fig. 5(a) show a large improvement for an RF tag with two antennas, with only slightly more for each additional antenna. Therefore, using two RF tag antennas is the best balance of RF tag footprint size and pinhole diversity gains. Furthermore, each RF tag antenna must be used to modulate backscatter; pinhole diversity gains and increased scattering aperture are not available to RF tags that use one antenna for communication and another to receive power.

2) Separate Reader Transmitter and Receiver Antennas: In Fig. 4, a comparison of PDFs with independent and fully correlated links shows that the correlated case is worse than that of independent links. Fully correlated links represent an extreme case that only occurs if a single reader antenna is used for both transmitting and receiving. Using separate, adequately spaced transmitter and receiver antennas avoids this problem.

3) Reader Transmitter and Receiver Arrays: As discussed in Section IV-C, great gains are available through the use of conventional antenna diversity at the reader. Hence, whenever cost effective, it is beneficial to use an antenna array at the reader receiver and transmitter to provide multiple diversity branches to a diversity combiner.

4) Increased Frequency: Most backscatter RF tag systems operate in the industrial, scientific, and medical (ISM) bands available at 902–928 MHz, 2400–2483.5 MHz, and 5725–5850 MHz in the United States. Though currently, the 902–928 MHz band is most common, several advantages are available to backscatter radio systems that operate in higher frequency bands, such as 5725–5850 MHz. In this band, RF tags with multiple antennas that experience uncorrelated fading are easier to design while maintaining a small tag footprint. In addition, this frequency band will allow reader antenna arrays to be

made very compact, and greater electrical separation between the RF tag antenna and the tagged object (due to the increased frequency) can improve antenna performance, especially on metal objects [20]. Operating in this band will likely cause 20 dB of excess path loss compared to the 902–928 MHz band [21], however, such losses can be reduced by the increased gain of the system at the higher frequency. As the power efficiency of passive RF tag ICs improve, operating in the 5725–5850 MHz ISM band will allow RF tags to be smaller and more reliable.

5) Backscatter Radio System Antenna Configuration: The backscatter radio communication benefits discussed in this paper can be realized using many types of antennas, but care must given in their implementation. At the reader, the elements of each array should be spaced to reduce fading correlation. The reader transmitter and receiver arrays should not be co-located [to avoid the fully correlated channel described by (7a)] and may be cross-polarized to help reduce self interference. On the RF tag, using cross-polarized antennas may reduce envelope correlation between signals scattered from each antenna. However, for both reader antenna arrays and RF tag antennas, the favorable correlation effects of cross-polarization must be balanced with the detrimental effects of unequal diversity branch power [9] caused by cross-polarization.

VI. CONCLUSION

The $M \times L \times N$ dyadic backscatter channel is a pinhole channel with deeper small-scale fades than a conventional one-way channel. Pinhole diversity can mitigate this fading by changing the shape of the fading distribution which, along with increased RF tag scattering aperture, results in up to a 10 dB gain at a BER of 10^{-4}. Examples have demonstrated that this gain leads to increased backscatter radio communication reliability and up to a 78% range increase. These gains require no channel knowledge or diversity combining at the reader, only the modulation of backscatter using multiple RF tag antennas and separate, adequately spaced reader transmitter and receiver antennas. Future research on this topic could include measuring the pinhole diversity gain in an actual dyadic backscatter channel, which will likely have a product Rician distribution.

APPENDIX
CHANNEL ENVELOPE PDF DERIVATION

The envelope PDF of the received signal can be derived from the PDF of the product of two dependent Rayleigh random variables [22][4]

$$f_\alpha(\alpha, \rho) = \frac{4\alpha \left(1 - |\rho|^2\right)}{\sigma_b^2 \sigma_f^2 M \gamma^2} \mathrm{I}_0\left(\frac{2\alpha|\rho|}{\sigma_b \sigma_f \sqrt{M}\gamma}\right) \mathrm{K}_0\left(\frac{2\alpha}{\sigma_b \sigma_f \sqrt{M}\gamma}\right) \quad (10)$$

for $\alpha > 0$. In (10), $\alpha = |\tilde{\mathbf{h}}^b| \times |\tilde{\mathbf{h}}^f|$, $\tilde{\mathbf{h}}^f \sim \mathcal{N}(0, M\sigma_f^2)$, $\tilde{\mathbf{h}}^b \sim \mathcal{N}(0, \sigma_b^2)$, and $\gamma = 1 - \rho^2$. The PDF of the sum of L i.i.d. random variables is the product of their characteristic functions (CF). The CF of (10) is found using the Hankel transform, which

---

raised to the Lth power yields the CF of the general $M \times L \times N$ dyadic backscatter channel

$$\Phi(\nu; \rho) = \left[\frac{\sigma_b^4 \sigma_f^4 M^2}{16} \frac{\gamma^4}{(1 - |\rho|^2)^2}\left(\nu^2 + \frac{4(|\rho| - 1)^2}{\sigma_b^2 \sigma_f^2 M \gamma^2}\right)\right.$$
$$\left. \times \left(\nu^2 + \frac{4(|\rho| + 1)^2}{\sigma_b^2 \sigma_f^2 M \gamma^2}\right)\right]^{-L/2}. \quad (11)$$

The PDF of (11) is found using the inverse Hankel transform.

REFERENCES

[1] H. Stockman, "Communication by means of reflected power," *Proc. I.R.E*, vol. 36, no. 10, pp. 1196–1204, 1948.
[2] K. Finkenzeller, *RFID Handbook: Fundamentals and Applications in Contactless Smart Cards and Identification*, 2nd ed. New York: Wiley, 2003.
[3] D. Kim, M. A. Ingram, and W. W. Smith, Jr., "Measurements of small-scale fading and path loss for long range RF tags," *IEEE Trans. Antennas Propag.*, vol. 51, no. 8, pp. 1740–1749, 2003.
[4] D. Chizhik, G. J. Foschini, and R. A. Valenzuela, "Capacities of multi-element transmit and receive antennas: Correlations and keyholes," *Electron. Lett.*, vol. 36, no. 13, pp. 1099–1100, 2000.
[5] D. Chizhik, G. J. Foschini, M. J. Gans, and R. A. Valenzuela, "Keyholes, correlations, and capacities of multielement transmit and receive antennas," *IEEE Trans. Wireless Commun.*, vol. 1, no. 2, pp. 361–368, 2002.
[6] V. Erceg, S. J. Fortune, J. Ling, A. J. Rustako, Jr., and R. A. Valenzuela, "Comparisons of a computer-based propagation prediction tool with experimental data collected in urban microcellular environments," *IEEE J. Select. Areas Commun.*, vol. 15, no. 4, pp. 677–684, 1997.
[7] D. Gesbert, H. Bölcskei, D. A. Gore, and A. J. Paulraj, "Outdoor MIMO wireless channels: Models and performance prediction," *IEEE Trans. Commun.*, vol. 50, no. 12, pp. 1926–1934, 2002.
[8] C. S. Patel, G. L. Stüber, and T. G. Pratt, "Statistical properties of amplify and forward relay fading channels," *IEEE Trans. Veh. Technol.*, vol. 55, no. 1, pp. 1–9, 2006.
[9] G. D. Durgin, *Space-Time Wireless Channels*. Upper Saddle River, NJ: Prentice Hall, 2003.
[10] M. Ingram, M. Demirkol, and D. Kim, "Transmit diversity and spatial multiplexing for RF links using modulated backscatter," presented at the Int. Symp. Signals, Systems, and Electronics, Tokyo, Japan, Jul. 24–27, 2001.
[11] M. Mi, M. H. Mickle, C. Capelli, and H. Swift, "RF energy harvesting with multiple antennas in the same space," *IEEE Antennas Propag. Mag.*, vol. 47, no. 5, pp. 100–106, 2005.
[12] D. M. Pozar, *Microwave Engineering*, 3rd ed. Hoboken, NJ: Wiley, 2005.
[13] J. D. Griffin and G. D. Durgin, "Link envelope correlation in the backscatter channel," *IEEE Commun. Lett.*, vol. 11, no. 9, pp. 735–737, 2007.
[14] W. C. Jakes, Ed., *Microwave Mobile Communications*. New York: IEEE Press, 1974.
[15] D. T. Auckland, W. Klimczak, and G. D. Durgin, "Maximizing throughput with ultra-compact diversity antennas," in *Proc. IEEE Vehicular Technology Conf. 2003-Fall*, Orlando, FL, 2003, vol. 1, pp. 178–182.
[16] Y. Yamada, K. Kagoshima, and K. Tsunekawa, "Diversity antennas for base and mobile stations in land mobile communication systems," *IEICE Trans.*, vol. E74, no. 10, pp. 3202–3209, 1991.
[17] J. D. Griffin, G. D. Durgin, A. Haldi, and B. Kippelen, "RF tag antenna performance on various materials using radio link budgets," *IEEE Antennas Wireless Propag. Lett.*, vol. 5, no. 1, pp. 247–250, 2006.
[18] P. Nikitin and K. V. S. Rao, "Performance limitations of passive UHF RFID systems," in *Proc. IEEE Antennas and Propagation Society Int. Symp.*, Albuquerque, NM, 2006, pp. 1011–1014.
[19] G. De Vita and G. Iannaccone, "Design criteria for the RF section of UHF and microwave passive RFID transponders," *IEEE Trans. Microw. Theory Tech.*, vol. 53, no. 9, pp. 2978–2990, 2005.
[20] J. T. Prothro, G. D. Durgin, and J. D. Griffin, "The effects of a metal ground plane on RFID tag antennas," in *Proc. IEEE Antennas and Propagation Society Int. Symp.*, Albuquerque, NM, 2006, pp. 3241–3244.

---

[4]Equation (10) differs from that given by Simon [22] in that it has been normalized to satisfy $\int_0^\infty f_\alpha(\alpha, \rho) d\alpha = 1$

[21] A. Affandi, G. El Zein, and J. Citerne, "Investigation on frequency dependence of indoor radio propagation parameters," in *Proc. IEEE VTC 1999*, 1999, vol. 4, pp. 1988–1992.

[22] M. K. Simon*, Probability Distributions Involving Gaussian Random Variables: A Handbook for Engineers and Scientists*. Norwell, MA: Kluwer Academic, 2002.

Joshua D. Griffin (S'00) received the B.S. degree in engineering from LeTourneau University, Longview, TX, in 2003 and the M.S. degree in electrical and computer engineering from the Georgia Institute of Technology (Georgia Tech), Atlanta, in 2005, where he is currently working toward the Ph.D. degree.

In 2004, he joined the Propagation Group at Georgia Tech where he researches microwave propagation and backscatter radio applications. In 2006, he participated in a three month research exchange program with the Sampei Laboratory, Osaka University, Osaka, Japan.

Gregory D. Durgin (S'96–M'01–SM'06) received the B.S.E.E., M.S.E.E., and Ph.D. degrees from Virginia Polytechnic Institute and State University, Blacksburg, in 1996, 1998, and 2000, respectively.

In 2001, he spent one year as a Postdoctoral Fellow with Morinaga Laboratory, Osaka University, Osaka, Japan. In Fall 2003, he joined the faculty of the School of Electrical and Computer Engineering, Georgia Institute of Technology (Georgia Tech), Atlanta, where he founded the Propagation Group (http://www.propagation.gatech.edu), a research group that studies radiolocation, channel sounding, direction finding, backscatter radio, RFID, and applied electromagnetics. He authored *Space-Time Wireless Channels* (Prentice Hall, 2002), the first textbook in the field of space-time channel modeling. He is also an active consultant to industry.

Dr. Durgin was co-recipient of the Stephen O. Rice Prize for Best Original Paper in the IEEE TRANSACTIONS ON COMMUNICATIONS in 1998, and was awarded a Postdoctoral Fellowship from the Japanese Society for the Promotion of Science (JSPS) in 2001. He was a winner of the NSF CAREER Award as well as numerous teaching awards, including the Class of 1940 Howard Ector Outstanding Classroom Teacher Award in 2007.